

The liquid Xenon set-up of the DAMA experiment

also ROM2F/2001-09 and submitted for publication

The liquid Xenon set-up of the DAMA experiment

R. Bernabei^a, P. Belli^a, A. Bussolotti^a, F. Cappella^a, R. Cerulli^a, C.J. Dai^b, A. Incicchitti^c, A. Mattei^c, F. Montecchia^a, D. Prospero^c

^a *Dip. di Fisica, Universita' di Roma "Tor Vergata" and INFN, sez. Roma2, I-00133 Rome, Italy;*

^b *IHEP, Chinese Academy, P.O. Box 918/3, Beijing 100039, China;*

^c *Dip. di Fisica, Universita' di Roma "La Sapienza" and INFN, sez. Roma, I-00185 Rome, Italy*

Abstract

The main features of the low background DAMA pure liquid Xenon scintillator set-up running deep underground in the Gran Sasso National Laboratory of the I.N.F.N. are described.

1 Introduction

Various detection strategies have been proposed for deep underground searches of Dark Matter particles. In particular we pointed out the interest in using liquid Xenon (LXe) as target-detector for WIMP search deep underground since ref. [1]. Several prototypes were built and related results published [2].

The choice to use liquid Xenon as a pure scintillator, directly collecting the emitted UV light, was performed because in this case no other material apart Xenon is present in the sensitive volume. In fact, this assures an improved radiopurity, a higher light response and the possibility of a pulse shape discrimination for electromagnetic background rejection [3]. A high radiopurity is also assured by the use of Kr-free Xenon gas, since the ^{85}Kr is a β^- emitter with a half life of 10.7 years.

Preliminary results were achieved both on elastic and inelastic WIMP- ^{129}Xe scattering [4, 5] by using Xenon gas enriched at 99.5% in ^{129}Xe . The response of a similar pure LXe scintillator to recoil nuclei as well as its pulse shape discrimination capability have also been measured [3]. Several upgradings of the set-up have been performed with time deep underground to improve its sensitivity, obtaining new results on the WIMP search [3, 6]. Several other rare processes have also been searched for by means of this set-up; results on charge non-conserving processes [7, 8, 9] as well as on the nucleon and di-nucleon stability [10] have been published.

At present the set-up is running filled with Kr-free Xenon gas enriched at $\simeq 68.8\%$ in ^{136}Xe , but the set-up configuration is such that the sensitive volume can be filled alternatively with Xenon gas enriched in ^{136}Xe or with Xenon gas enriched in ^{129}Xe .

In this paper the main features of the low background DAMA pure liquid Xenon scintillator set-up are reviewed.

2 Liquid Xenon as scintillator

A detailed description of the main characteristics of liquid Xenon as a detector medium considering scintillation, ionization and proportional scintillation properties was given in refs. [11, 12]. In the following we recall only main physical properties useful for its application as regards direct scintillation.

The scintillation is produced through the processes summarized in Fig.1, where excited atoms R^* and ions R^+ produced by ionizing radiation are involved. Here $h\nu$ is an ultraviolet photon having $\lambda = 178\pm 1$ nm [13] with a bandwidth of $\Delta\lambda = 14\pm 2$ nm as measured at 160 K in presence of a contamination level in N_2 , H_2 and rare gases $< 0.01\%$. An extensive study of the optical properties of condensed Xenon was performed in the period 1960-1970[14].

Because the scintillation emission is in the far-UV region, an efficient light transmission and collection is a fundamental point for a LXe scintillator. Impurities that absorb UV light (such as Nitrogen, water, hydrocarbons etc.) could act as an inefficient wave shifter or as quenchers degrading the light response. Therefore a particular care has to be devoted

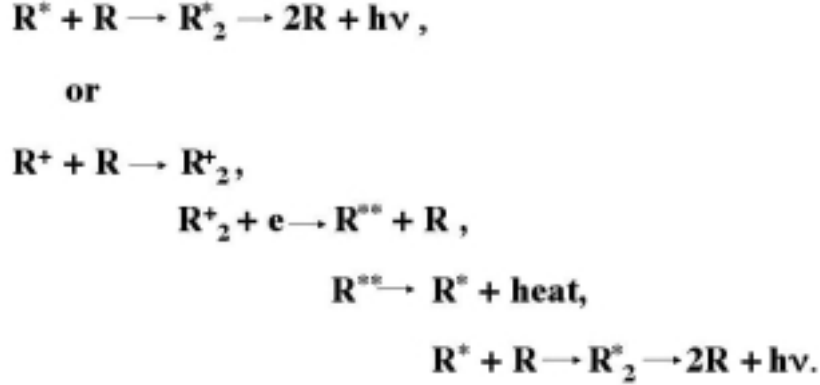


Figure 1: Scintillation processes in liquid Xenon.

to the purification of the used Xenon and to the choice of materials that enter in direct contact with it. These requirements, in case of experiments searching for possible rare processes, have to be matched with the necessity to use low radioactivity materials in order to reduce as much as possible the background.

As regards scintillation, first indications that liquid Xenon could approach NaI(Tl) in light output date back to 1958[15]. In particular the high atomic number, the high density and the scintillation efficiency similar to those of NaI(Tl) have been increased the interest in this scintillator for different fields of application, due also to its fast response and to the estimated high tolerance to radiation damage. Some numbers of comparison with NaI(Tl) are given in Table 1.

Table 1: Few numbers of comparison between LXe and NaI(Tl) scintillators. The data marked with (*) are referred to LXe at 179 K, in case of electron excitation and electric field of 4 kV/cm applied[16].

	Liquid Xe	NaI(Tl)
density (g/cm ³)	3.06 at boiling point	3.67
Fast decay time τ_1 (ns)	2.2*	230
Slow decay time τ_2 (ns)	27*	—
A_1/A_2 ratio	0.6*	
Ratio α/e	1.1±0.2	0.5–0.6
(Birks' constant) ⁻¹ (MeV/cm)	30600	3670
(dE/dx) _{min} (MeV/cm)	3.9	4.85

The scintillation from liquid Xenon has two decay components (see Table 1) corresponding, respectively, to the life time of singlet and triplet state of the excited molecule.

An additional decay component (with decay time τ_r) can be considered in order to take into account the recombination[17, 18] between electrons and ions. In case of electron excitation the time τ_r is longer than τ_1 and near to τ_2 ¹. In case of alpha particle excitation, the recombination process is instead fast due to the high density of ionization. The recombination effect does not appear when a strong electric field is applied. We recall in particular that an α/e light ratio $\simeq 1.1 - 1.2$ has been measured by various authors in pure LXe scintillators (see e.g. refs.[2, 20, 21, 22] for details) showing the important role that recombination can play in liquid Xenon.

A relevant quantity, when scintillation is considered, is the mean energy needed for producing a scintillation photon, W_s . Various measurements and estimates are available in literature for different types of initial particles as shown in Table 2. Detailed comments can be found in ref.[21].

Table 2: Theoretical estimates and experimental measurements of W_s (eV) for LXe scintillators. For comparison we recall that $W_s \simeq 23$ eV in NaI(Tl).

Liquid Xenon	Relativistic electrons	α particles	Relativistic heavy particles
Theoretical[21]	$23.7^{+5.8}_{-6.3}$	19.6 ± 2.1	$14.7^{+1.5}_{-3.3}$
Experimental	< 35 [23] 67 ± 22 [24] 29.6 ± 1.8 [2] 14.2 [26]	16.3 ± 0.3 [20] 39 [25]	

For completeness, we recall that an important point, as regards the search for dark matter particles, is the light response versus the released energy in case of a WIMP-nucleus scattering; see sect. 4.2 for some details.

As regards measurements of the scintillation light attenuation length in liquid Xenon we refer to ref. [2] and refs. quoted therein.

The diagram of state of Xenon is given in Fig. 2. A deep stability and control of the thermodynamical working conditions and in particular of the uniformity with which these conditions are reached is fundamental in order to have a good and stable light collection.

Finally, as regards the refractive index it has been quoted to be 1.7 at 170 nm, while it decreases to 1.4 at 360 nm (where liquid Xe is considered at 173.2 K and 1 atm) [19]. Some estimates can be found also in ref. [27].

¹In this case $\tau_r = 45$ ns and $A_2/A_r = 0.6$. In terms of intensity, considering $i(t) = A_1 e^{-t/\tau_1} + A_2 e^{-t/\tau_2} + A_r e^{-t/\tau_r}$ with $\int_0^\infty i(t) dt = 1$, it follows $I_1 = 0.01$, $I_2 = 0.25$ and $I_r = 0.74$ where $I_k = \int_0^\infty A_k e^{-t/\tau_k} dt$ with $k = 1, 2, r$, as quoted in ref.[19]

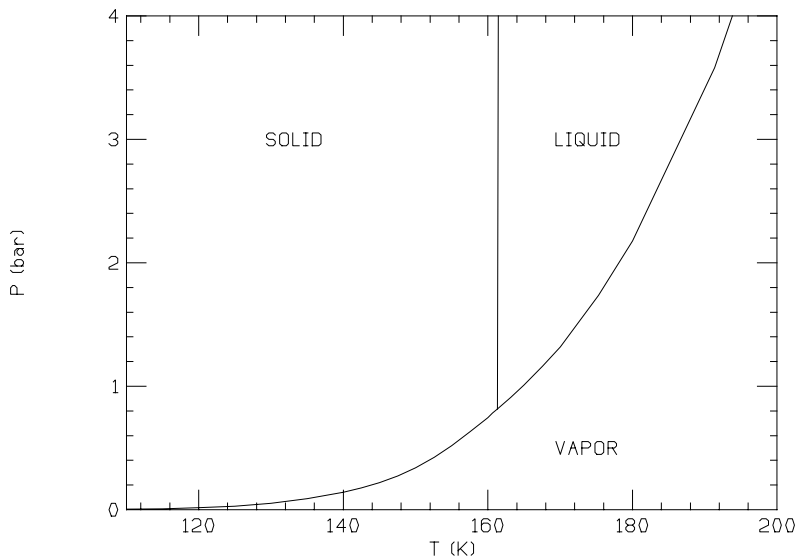


Figure 2: Diagram of state of Xenon.

3 The experimental set-up

The DAMA LXe experimental set up is running deep underground at the Gran Sasso National Laboratory of the I.N.F.N. since several years and various upgradings to improve its performance and sensitivity have been carried out with time; the latest one has been performed in August 2000.

The main parts of this set-up (see Fig.3 and 4) are: i) the inner vessel where the Xenon undergoes to the transition between the gaseous and the liquid phase; ii) the external vessel where the insulation vacuum is made and where are located three photomultipliers which collect the UV light through the optical windows of the inner vessel; iii) the shield; iv) the cryogenic system constituted by a He compressor which drives a one-stadium cold head and a cryo-pump; moreover an heater and a turbomolecular pump are also operative; v) a vacuum/filling/purification/recovery system for the Xenon.

The whole installation is under air conditioning and this assures the utmost stability conditions on environmental temperature in order to avoid any possible influence on the working conditions. The electronics and the acquisition system (DAQ) are placed on the upper floor of the building, which is also air conditioned.

3.1 The inner vessel

The sensitive volume of the inner vessel is of $\simeq 2$ l, corresponding to $\simeq 6.5$ kg of liquid Xenon. The inner vessel is made by highly radiopure OFHC Copper and its external shape is a parallelepiped with squared base. The inner volume has been excavated in a particular shape to optimize the light collection (that is avoiding the presence of any "dead region") through the optical windows present on three of the lateral faces of the parallelepiped. Three CONFLAT flanges assure the connection with the 10 cm in diameter optical windows made of cultured crystal quartz. They are bakeable up to 200 $^{\circ}$ C. The

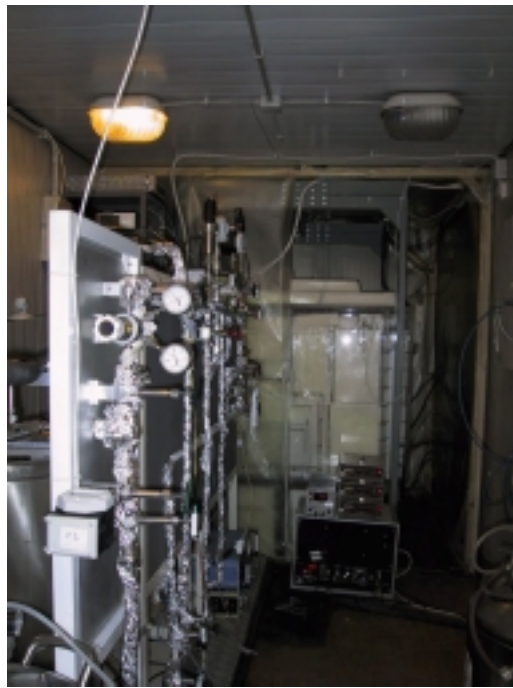


Figure 3: A view of the vacuum/filling/purification/recovery system; the shield of the set-up is visible in the bottom.



Figure 4: A view of the inner vessel.

optical windows offer a transparency of about 80% (including reflection losses) to the UV emission ($\lambda \simeq 178$ nm) of the LXe pure scintillator. The mechanical features of these windows assure the possibility to safely work with Xenon gas at about 2 bar pressure

during the liquefaction. An UHV valve (electropolished, all metal, bakeable) directly connected to this vessel allows an independent and direct way for its evacuation and the possibility to insert a particular home made getter, that can work directly in the liquid Xenon. An upper flange allows the connection with a stainless steel tombak to insert the radioactive source for the calibration.

The temperature monitoring of the inner vessel is performed by a Lakeshore system having four miniaturized semiconductor sensors placed inside holes along the Cu vessel and an external controller.

The leakage of this vessel was tested to be less than 10^{-9} mbar·l·s⁻¹.

Further details on specific solutions chosen for the UHV connections and the thermic link are given in sect. 3.6.

3.2 The external vessel and the shield

The external insulation vessel is a 316 stainless steel cylinder (about 100 l volume). It has various vacuum feedthroughs and flanges in order to work on photomultipliers, cold head, sensors, etc..

The shield is made with 5-10 cm of low radioactive copper inside the vacuum insulation vessel (to shield, at the most, mainly possible background contribution from PMTs), 2 cm of steel (wall of the insulation vacuum vessel), 5-10 cm of low radioactive copper, 5 cm of Polish lead and 10 cm of Boliden lead, \simeq 1 mm Cadmium and \simeq 10 cm of polyethylene plus paraffin with a thickness fixed by the available space. The Cadmium and the polyethylene/paraffin are used to shield the set-up from environmental neutrons; measurements on neutron fluxes deep underground in the Gran Sasso National Laboratory — in the various energy regions — can be found for example in ref. [28]. Finally, an external plexiglass box, sealed and fluxed with HP Nitrogen closes the external shield.

3.3 The vacuum and cryogenic system

The vacuum/filling/purification/recovery system has electropolished 316L stainless steel tubes with VCR fittings and valves (electropolished, all metal, bakeable). A schematic view is given in Fig.5.

An ultra high vacuum, UHV, (typically not worst than 10^{-6} mbar) is required for the vacuum/filling/purification/recovery line and for the inner vessel, while less stringent requirements are needed for the insulation chamber (typically not worst than 10^{-3} mbar). In this chamber the vacuum is produced by a turbomolecular pump and read out by a Pirani gauge through a LEYBOLD controller mod. IG3 that gives a logarithmic analogic output (0 - 10 V full scale) and an output as NC contact (normally closed) for alarm and monitor. This control allows to pilot an electropneumatic valve that can close the insulation vacuum line, in order to trap the Xenon gas in case of accidental break of the cultured crystal quartz windows.

The UHV for the inner vessel and the vacuum/filling/purification/recovery line is firstly produced by a LEYBOLD turbomolecular pump and, secondly, by a LEYBOLD

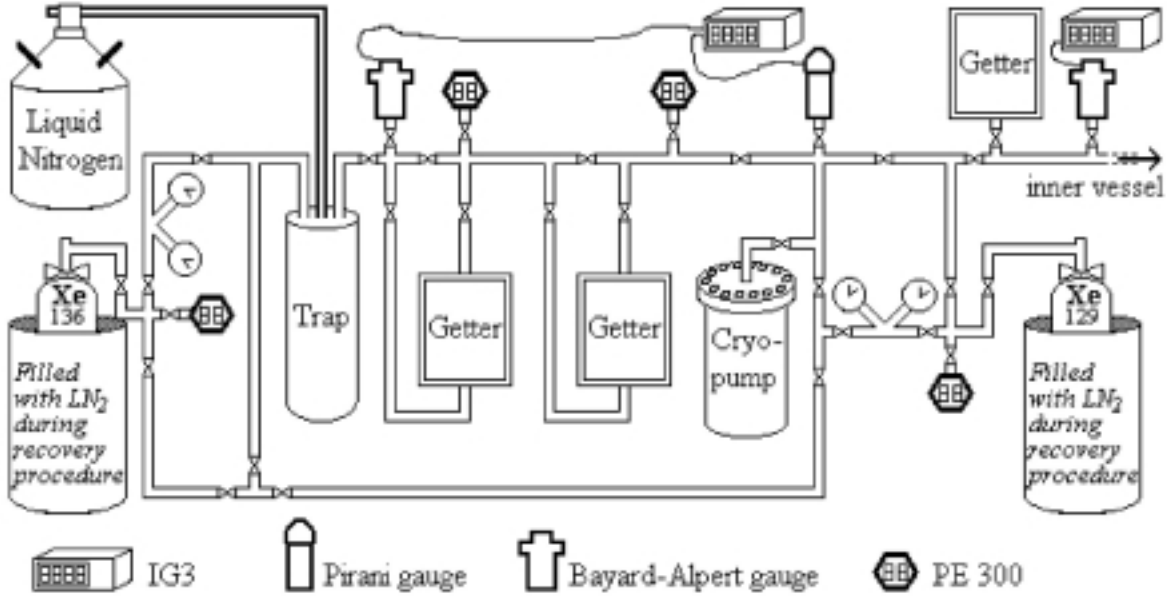


Figure 5: Schematic view of the vacuum/filling/purification/recovery line

cryo-pump mod. RPK 900 (at 20 K). Part of the vacuum procedure is executed at 160 °C for a long time. The UHV is read out by two Bayard-Alpert gauges through two LEYBOLD mod. IG3. On the line also a bakeable Pirani gauge is connected. All the line has a leakage less than 10^{-9} mbar·l·s⁻¹.

An Helium compressor LEYBOLD mod. RW 5000 (located outside the experimental site in a concrete container specially equipped in the internal part to avoid any vibration) pilots the cold head (LEYBOLD mod. RGS120 single stadium 80 K) and the cryo-pump. The stable working temperature to keep liquid the Xenon is obtained with a heater directly connected to the cold head. The temperature on the cold head is monitored with a PT100 sensor. During normal run conditions a voltage (relative stability of $2 \cdot 10^{-4}$) is supplied to the heater to maintain stable the operating temperature. During the recovery procedure of Xenon (for which higher voltage and higher current are needed) a LEYBOLD mod. HR1 controller, properly modified for our use, allows to gradually heat the inner Xenon vessel. A suitable thermic link made of low radioactivity OFHC copper connects the Xenon vessel to the cold head/heater system. The cold head is supported by a suitable basement that protects the apparatus from any vibration noise.

The compressor as well as the turbomolecular pump, is water cooled and its correct operation must respect fixed parameters of capacity and temperature of the water. In particular, a tank of water outside the experimental site is operative for the cases of lack of the current water. The water circulates through two twin circuits (in order to at least guarantee the operation in case of breakdown) and is normally replaced from current water at the actual capacity of job of 7 l/min. The temperature (T1) of the outgoing water at the exit of the compressor unit is controlled through a sensor dipped in the water itself; it is an integrated sensor of National Semiconductor LM35 that can work between

-40 and 100 °C with a linear output of 10 mV/°C.

The control on the correct working conditions of the compressor unit is performed by a LEYBOLD sensor inside the system with a remote control through a 24V d.c. output transformed in a NC contact. In an analogous way the compressor unit supply is monitored.

This cooling/heater system was preferred to other systems less expensive (as possible with cold baths) because it can guarantee a high level of thermodynamical stability. The temperature of the liquid Xenon has typically a stability of 0.1 °C over one month of work.

As regards the purification system firstly it is used a cold Nitrogen trap whose working temperature is set and monitored by a temperature controller (typically 190 K). It purifies Xe from possible Rn, H₂O and other impurities that condense at this temperature. It is used during the full procedure of gas filling and liquefaction. Moreover, a Monotorr getter by SAES and home-made getters allow, each one, outlet impurities < 1 ppb for any component: O₂, N₂, CO, etc. [29]. The getters are firstly activated at 400 °C and then used at different and/or environmental temperature during the liquefaction procedure and run conditions. One getter in liquid phase can also be used.

The used Xenon gas is Kr-free enriched Xenon (two options are possible at present: enrichment at 99.5% in ¹²⁹Xe or enrichment at 68.8% in ¹³⁶Xe). Two lines of filling/recovery allow the separate use of the two gases. The liquefaction and recovery procedures are performed slowly in order to avoid thermic stress on optical windows and photomultipliers. During the filling procedure for a given temperature we maintain higher pressure with respect to the equilibrium line (see Fig. 2) between liquid and vapor in the diagram of state. The pressure in any case for safety reasons is kept \lesssim 2 bars.

When the liquefaction procedure is completed and the stability in temperature is reached, giving a suitable constant voltage supply to the heater, the Xenon vessel is insulated and kept in direct contact only with getters. Therefore temperature and pressure move along the equilibrium curve. In this way we can take advantage of a large plateau of work, typically in the range between 168 and 178 K. Lower temperatures are not preferred again to avoid stress on photomultipliers.

The stainless steel bottles of Xenon are inserted in stainless steel dewars. When the recovery procedure of the used Xenon gas starts, the corresponding dewar is filled with liquid Nitrogen and the Xenon is gradually stored back in its bottle while the Xenon vessel is heated.

3.4 The photomultipliers

Three 3.5" of diameter flying leads photomultipliers with Magnesium Fluoride windows collect the scintillation light through the cultured crystal quartz optical windows. The photomultipliers used in this experiment were specially realized with the peculiar requirements of UV light collection and maximization of quantum efficiency at the UV wavelength of interest. The photomultipliers are EMI D631/FL, that is without sockets. Their flying leads are directly connected to suitable voltage dividers with miniaturized SMD resistors

and capacitors (whose low radiopurity has also been measured by Ge detector), mounted on thin teflon sockets. The solders have been performed by using low radioactive Boliden lead and low radioactive resin. The voltage dividers have also been optimized to reach the best signal/noise ratio; a sketch is shown in Fig. 6. The PMTs work near the maximum

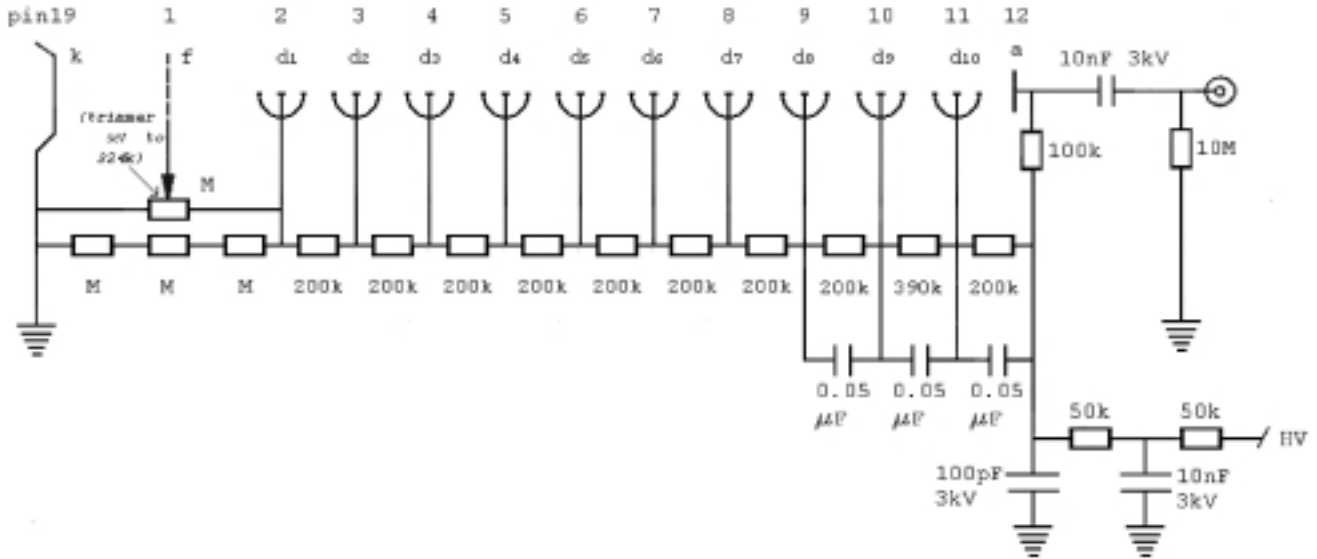


Figure 6: The voltage divider.

high voltage — within the linearity plateau — in order to assure a suitable energy threshold. The PMTs have ten dynodes with linear focus, their measured quantum efficiency — for normal incidence — ranges between 18% and 32% at the LXe scintillation wavelength with a flat behaviour around the measured value; moreover, they have good pulse height resolution for single photoelectron pulses, low dark noise rate and a gain of $\approx 10^6 - 10^7$. The three PMTs work in coincidence at single photoelectron threshold.

3.5 The electronic chain

The three photomultipliers have grounded cathode supplied by positive high voltage. The voltage suppliers have a stability of 0.1%. Each photomultiplier is connected to a low noise preamplifier with a 0-250 MHz bandwidth range, with a voltage amplification of ten and with an integral linearity of $\pm 0.2\%$. Particular attention has been paid to the low voltage power system in order to limit at the most possible electronic noise.

A schematic drawing of the electronic chain is shown in Fig. 7.

The amplified signals of the three PMTs — by means of Linear Fan-in Fan-out — provide: i) the inputs of the sum of the three pulses; ii) a signal to the charge ADC in order to record the pulse energy collected by each side only (for possible single/sum correlation analysis); iii) the inputs of three timing filter amplifiers with 50 ns integration time. The subsequent discriminators have triggers at photoelectron level.

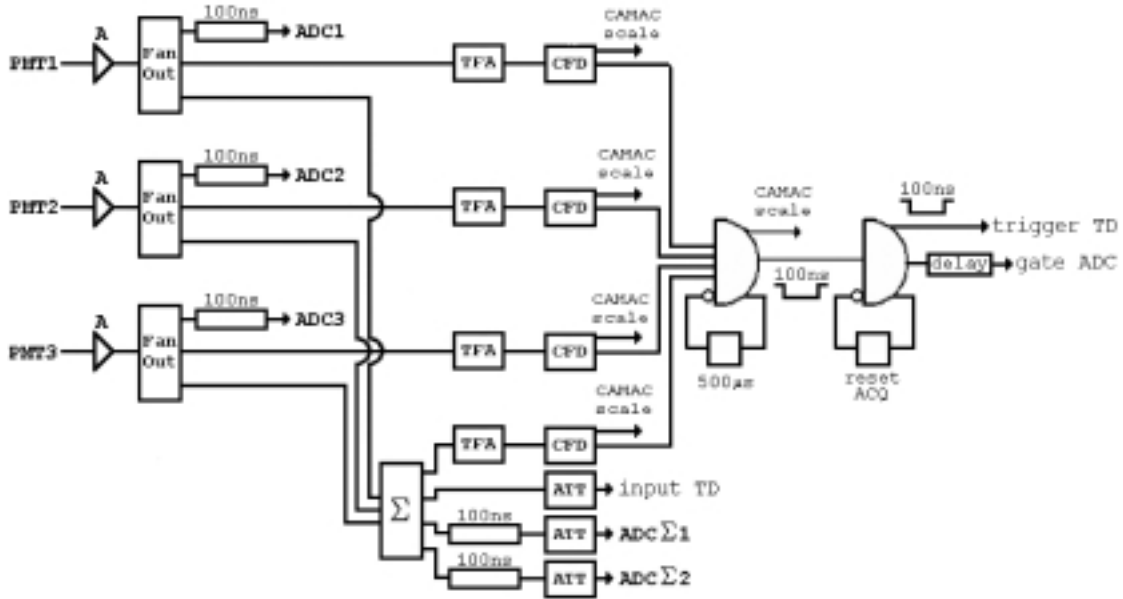


Figure 7: Schematic view of the electronic chain.

The summed signal of the three PMTs is splitted by a Linear Fan-in Fan-out and is addressed to: i) a Transient Digitizer LeCroy 8828D with a digitizing sampling rate of 200 MS/s recording the pulse shape in a 1000 ns time window; ii) a charge ADC with a scale suitable for low energy; iii) a charge ADC — after 22 db attenuation — suitable for events in the intermediate-energy range; iv) a timing filter amplifier and a discriminator with threshold at single photoelectron level.

The detector trigger requires the coincidence of the four logical signals: from the three PMTs and from the sum. A Gate Generator rejects events occurring within a time window of 500 μ s after event collection; this requirement introduces a negligible relative systematic error. A subsequent coincidence takes into account the busy signal from data acquisition in order to give the correct trigger to the Transient Digitizer and the gate of 100 ns to the ADCs with a suitable circuit to avoid triggers during the acquisition time of an event. The corresponding dead time is evaluated by comparing the hardware triggers and the acquired triggers; it is typically of a few per cent. The data acquisition is performed by a CAMAC system. For each event the following informations are recorded: amplitudes of each single PMT pulse; amplitudes and shape of the sum pulse (recorded by the Transient Digitizer).

Finally, we note that an upgrading of the electronics is in preparation in order to have in near future a Transient Digitizer on each photomultiplier and in order to introduce a passive power splitter - before the signal enters in the preamplifier - to allow in the same run the collection of higher energy signals by ADC.

3.6 The radiopurity

The inner vessel, the surrounding insulation vessel, the thermic link, the vacuum/filling/-purification/recovery line, etc. were realized with materials selected for low radioactivity mainly by sample measurements with Ge detector deep underground in the Gran Sasso National Laboratory (LNGS). Most of the detector and of the shield materials as well as the used Xenon gases have been kept deep underground since many years.

The internal vessel is made by OFHC low radioactive copper. This detector has the unique feature that no O-rings were used for the flanges connected to it (windows, vacuum/filling tube etc.), the stainless steel material was minimized and the Cu itself acts as O-ring in all the connections steel/Copper. This was obtained matching a suitable inclination of the knife on the stainless steel flange with the tight of the screws. Where a connection Copper/Copper was needed, as for the upper flange of the internal vessel (see Fig. 4) this was obtained by using a sandwich structure Copper/steel/Copper with a thin stainless steel ring. Also the thermic link was performed all with low radioactive OFHC Cu without any additional material (such as Indium etc. normally used).

Results on residual radioactivity in materials nearby the LXe sensitive volume are given in Table 3.

Table 3: Residual radioactivity in materials nearby the LXe sensitive volume measured with various techniques; the limits are at 95% C.L.

Materials	^{238}U	^{232}Th	^{nat}K
Cu vessel	<16 ppt	< 16 ppt	< 10 ppb
Cultured crystal quartz	—	<6 ppb	<11 ppm
Stainless Steel	< 3 ppb	< 10 ppb	<33 ppm

In our set-up Kr-free Xenon gas enriched in ^{129}Xe at 99.5% by ISOTECH company has been used. The enrichment was verified at the arrival of the Xenon bottle by mass spectrography[30, 31]. Since August 2000 the vessel can also alternatively be filled with Kr-free Xenon gas enriched in ^{136}Xe at 68.8% by Oak Ridge [32, 33]². Both the Kr-free enriched gases are deep underground since many years.

Due to the enrichment procedure, giving the separation from Kr, the radiopurity of the gas is hugely increased with respect to natural Xe. Moreover, only Xenon radioactive isotopes with very short half-life exist; the longest half-life isotope is ^{127}Xe with 36.41

²The choice to consider enrichments in these two particular Xenon isotopes lies on the scientific purpose of the experiment. In fact, in case spin dependent coupled WIMPs are searched for, the enrichment in ^{129}Xe increases of about a factor 3 the target mass with respect to natural Xenon and – in addition – the ^{129}Xe offers a higher spin factor with respect to other targets with exception of ^{19}F . The present availability also of the Kr-free Xenon gas enriched at 68.8% in ^{136}Xe allows to perform data taking in the same set-up with a target once sensitive and once not to spin-dependent coupled WIMPs as well as to investigate the $\beta\beta$ decay of ^{136}Xe .

Table 4: Isotopic composition of the Xe enriched in ^{129}Xe and original (before first purification cycle) content of trace contaminants[30, 31].

^{129}Xe	99.5 %
^{128}Xe	(0.25 ± 0.05) %
^{130}Xe	(0.25 ± 0.05) %
O_2	< 3 ppm
N_2	< 5 ppm
H_2	< 2 ppm
H_2O	< 3 ppm
hydrocarb.	< 1 ppm
Kr	< 0.02 ppm
CF_4	< 1 ppm
CO_2	< 1 ppm

days. The other Xe isotopes have very fast decay time and their possible cosmogenic presence can be removed after few months of storage deep underground.

In Table 4 and 5, respectively, the isotopic composition of the Kr-free enriched Xenon gases used in our set-up are given. For the first case also the original (before any purification cycle) content of trace contaminants is given, while for the second one it is not available here. For comparison we recall that e.g. natural Xe of 99.998% purity commercially available typically contains > 400 times higher Kr concentration.

Table 5: Main isotopic composition of Xe enriched in ^{136}Xe [32, 33]; the original (before first purification cycle) content of trace contaminants is not available here.

^{136}Xe	68.8 %
^{131}Xe	2.9 %
^{132}Xe	8.5 %
^{134}Xe	17.1 %

The radiopurity of the purification system was also deeply investigated. As regards the cold Nitrogen trap the only part directly in contact with Xenon is the spiral electropolished stainless steel tube where it goes through. Moreover, due to the strong contamination of Rn in Oxisorb (see Table 6), after some tests, we chose to avoid its use preferring the use of getters. The alloy St707 (see Table 6), used in our getters, is a suitable material for radiopurity considering also that we can use getters in cascade at different temperatures. In addition the getters' material is assembled in electropolished housing by SAES or by us and can be equipped with a PALL microfilter (removal rating >0.003 μm) with electropolished 316L stainless steel housing, no O-ring and all fluoropolymer Super-Cheminert element[34]. The material of the home-made getters is originally available in form of pills sealed in Nitrogen atmosphere.

Table 6: Residual radioactivity in oxisorb (not used in the DAMA low background LXe scintillator) and in getters as measured at the LNGS with the low background Ge detector; the limits are at 95% C.L.

Materials	^{238}U (ppb)	^{232}Th (ppb)	^{nat}K (ppm)
Oxisorb	298 ± 33	431 ± 9	24 ± 5
St707	< 25	< 10	< 7

As regards the residual contamination in the used PMTs whose characteristics were largely fixed by the previously mentioned requirements, measured values for main parts are given in Table 7.

Table 7: Residual radioactivity in PMT components as measured at the LNGS low background facility with the low background Ge detector; the limits are at 95% C.L.

Materials	^{238}U (ppb)	^{232}Th (ppb)	^{nat}K (ppm)
MgF ₂ window	—	< 10	< 20
Dynodes	< 50	< 50	< 200

As described before, to keep the thermic insulation the external vessel is under vacuum. Moreover, Copper bricks are used to fulfil this chamber as much as possible to act as shield mainly from possible background contribution from PMTs. This chamber is surrounded by the external shield and by a plexiglass box that is continuously fluxed with HP Nitrogen gas and kept in small overpressure with respect to the environment. This assures the insulation from the environmental air, which contains radon in traces. The ^{222}Rn ($T_{1/2} = 3.82$ days) and ^{220}Rn ($T_{1/2} = 55$ s) isotopes from ^{238}U and ^{232}Th chains, respectively, are in gaseous form and their daughters attach themselves to surfaces by various processes. In underground laboratories, ^{222}Rn and ^{220}Rn are due mainly to decays in the rocks and accumulate themselves in closed spaces. Therefore, in rare event searches any contact between the detectors and the environmental air has to be avoided in order to reduce both the background counting rate and the permanent pollution of the detector surfaces. These requirements are important not only in running conditions but also in all the procedures followed during the assembling of the full set-up.

The radiopurity characteristics of the shield are given in Table 8. Before the installation, the lead bricks have chemically been etched by HNO₃ aqueous solution and the Cu bricks – as all the Cu parts of the set-up – by HCl aqueous solution; the used water was extremely radiopure. Before the installation of the external plexiglass box, a Supronyl (permeability: $2 \cdot 10^{-11}$ cm²/s[35]) envelop — fluxed with HP N₂ — wrapped the shield.

For sake of completeness we recall that energy distributions in various regions have been published several times; for recent results with ^{129}Xe before the latest upgrading see refs.[3, 6, 10]. In particular, we have measured there in the region of interest for

Table 8: Measurements of the residual radioactivity in some components used in the passive shield as performed at the LNGS low background facility with the low background Ge detector; the limits are at 95% C.L.

materials	^{238}U (ppb)	^{232}Th (ppb)	^{nat}K (ppm)
Cu bricks	<0.5	< 1	<0.6
boliden Pb	<8	<0.03	<0.06
boliden2 Pb	<3.6	<0.027	<0.06
polish Pb	<7.4	<0.042	<0.03
polyethylene	< 0.3	<0.7	<2
Plexiglass	<0.64	<27.2	<3.3

WIMP search upper limits on recoils (90% C.L.) ranging from $\simeq 0.4$ down to $\simeq 10^{-2}$ cpd/kg/keV[3] and a counting rate $\lesssim 10^{-4}$ cpd/kg/keV above 250 keV[6, 10]. New data taking is in progress.

4 Calibrations

4.1 Calibration with γ source

The energy calibrations in keV electron equivalent unit are typically performed with a ^{109}Cd (peaks at 22 and 88 keV) isotope by Amersham. It is sealed in a small stainless steel capsule with a thin window ($\simeq 190 \mu\text{m}$) suitable to work in the operative conditions of our set-up (ultra high vacuum, low temperature and high pressure of Xe). The source is supported by a tombak (15 cm linear motion) which can vary its vertical position and is normally placed in a central position inside the inner vessel when it is evacuated; so the source is already inside during the Xe liquefaction phase.

The typical response of the low radioactivity LXe scintillator to bare ^{109}Cd isotope is shown in fig. 8. The energy dependence of the detector results: $\frac{\sigma}{E} = 0.056 + \frac{1.19}{\sqrt{E[\text{keV}]}}$.

In the data analysis a software energy threshold of 13 keV (the hardware threshold is at single photoelectron level) has been considered so far to reject at the most any possible contribution from the tail of PMT noise pulses. Procedures to discriminate, at very low energy, noise pulses from LXe scintillation pulses cannot effectively be pursued because of the slight difference in the timing structure of the two kinds of pulses. In fact, the scintillation decay time of LXe is relatively fast and the available number of photoelectrons/keV is relatively modest.

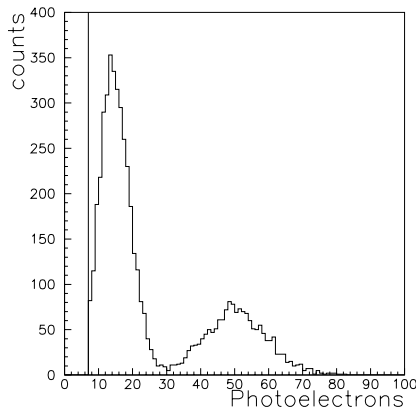


Figure 8: Response of the low radioactivity LXe scintillator to bare ^{109}Cd isotope.

4.2 Calibrations with neutrons

To obtain the energy of a recoiling nucleus in keV from its value in keV electron equivalent (as given by γ source calibrations) is necessary to measure the ratio of the amount of the light induced by a recoiling nucleus to the amount of light induced by an electron of the same kinetic energy. This quantity is usually named quenching factor, q , in the particle Dark Matter field. Often q expectations are estimated by considering the so called Lindhard theory [36]; however, the latter does not account for all the processes which can occur in every kind of detector. In particular, in a pure liquid Xenon scintillator q is enhanced with respect to estimates by Lindhard theory mainly because of the recombination effect in LXe (see sect. 2). However, the amount of such an enhancement - in operating conditions - depends on various specific experimental features, such as e.g. on the initial purity of the used Xenon gas, on the inner surface treatment, on the reached vacuum before filling, on the used purification line components and on the degassing/release characteristics of all the materials of- and inside- the inner vessel since some specific trace contaminants can act as quenchers for the scintillation light.

Since the use of neutron source in a low background installation is forbidden by the consequent activation of the irradiated materials, neutron calibrations have been performed by using a 40 cc detector especially built for this purpose [3]. They have been carried out both by the method of ref. [37, 38] with an Americium-Boron (Am-B) neutron source (obtaining a value averaged between 10 and 50 keV: $q_{<10-50\text{keV}} = 0.65 \pm 0.10$) and by detecting scattered neutrons at fixed angles using the ENEA-Frascati neutron generator giving about 14 MeV neutrons[39] (obtaining a value averaged between 150 and 230 keV: $q_{<150-230\text{keV}} = 0.45 \pm 0.12$). Although a certain dependence on energy can be expected for q , since the two determinations agreed within the errors, cautiously the overall mean value and the half dispersion have been calculated: 0.55 ± 0.11 (maximal error) and the most cautious value 0.44 has been considered since then when evaluating

results on WIMP searches. For details see ref. [3]³. To complete the program on neutron data taking, at the end of 2000 we have performed further measurements at the ENEA neutron beam with neutrons of 2.5 MeV; a dedicated paper is in preparation.

The neutron measurements have also allowed a quantitative investigation of the possibility of a pulse shape discrimination between electromagnetic background and Xenon recoils after preliminary studies on the different decay times between α and electron pulses[2, 42]. The results have been described in ref. [3].

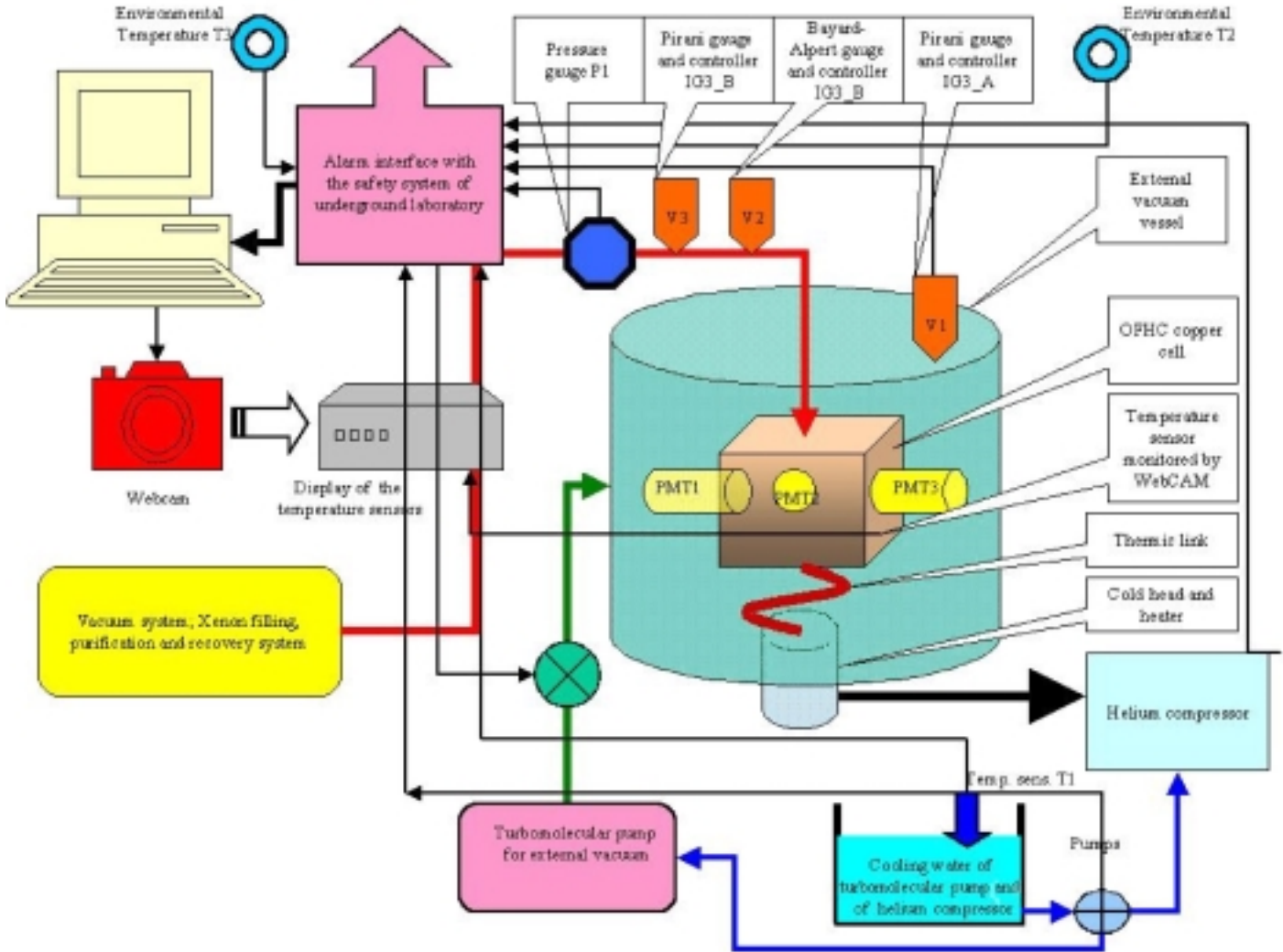


Figure 9: The alarm system.

³For the sake of completeness we recall that it has been recently presented in ref. [40] and in [41] a q value at level of pure Lindhard expectation in liquid Xenon detector. In both case the set-up was significantly different as regards the previously mentioned operating and characteristic features from our one.

5 Monitoring of sensors and alarm system

The main control parameters are the pressure and the temperature of the Xenon vessel. To monitor them a high precision temperature sensor with an external display (as mentioned in sect. 3.1) and a pressure sensor DIGIBAR mod. PE 300 (-1,10 bar) are used.

As already mentioned, on the inner vessel four temperature sensors are working, while two pressure sensors are active on the Xenon line next to the inner vessel; however, in Fig. 9 only the two (one for temperature and one for pressure) used for the remote control are pointed out.

The sensor values are continuously monitored with time by a PC (see Fig. 9) with an internal board National Instruments mod. PC-LPM16 PnP having 16 analogic inputs for an ADC with 12 bit resolution and range from +5V a -5V. By LabView software, a program that manages monitoring data and presents a front panel with their values during each run of data taking has been developed. In Fig.10 the front panel during a run is shown.

To allow a remote control of the experimental conditions a web site has been created to monitor all the needed parameters. In particular, a WebCam has been installed and interfaced with the Web server in order to show in real time (2 minutes resolution) the display of a sensor (see Fig.11) which cannot be accessed by electronic devices and whose substitution would require a large dismounting of the set-up.

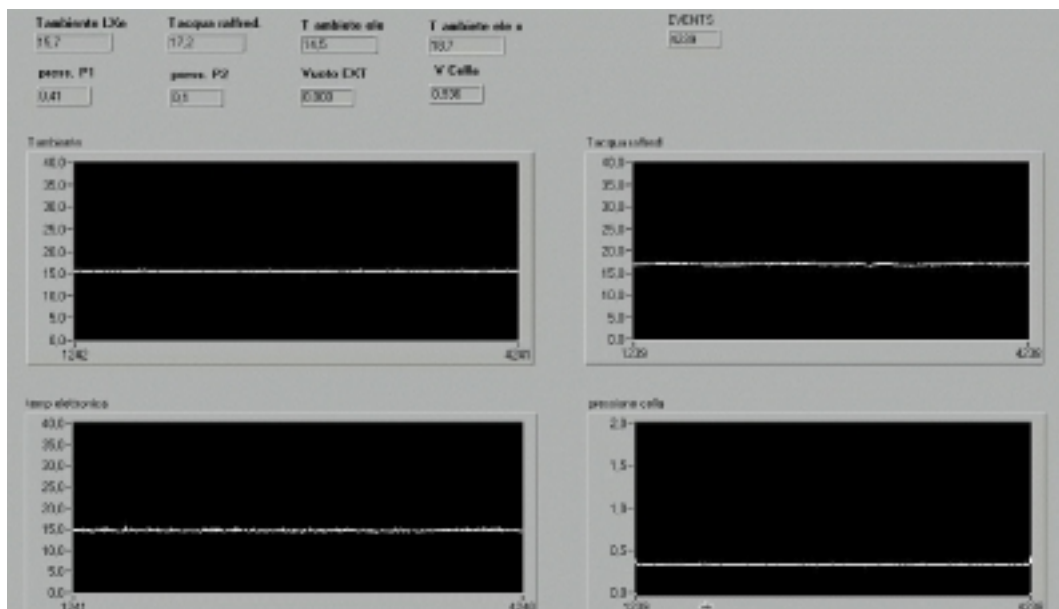


Figure 10: Display of the behaviour of sensors values in running conditions. Top left: the environmental temperature ($^{\circ}\text{C}$); top right: the temperature ($^{\circ}\text{C}$) of the cooling water when outgoing from the compressor unit; bottom left: the temperature of the electronics ($^{\circ}\text{C}$); bottom right: the LXe vapor pressure with respect to external pressure.



Figure 11: WebCam image of: top - the external vacuum IG3 display as measured by Pirani gauge (end scale is shown); bottom - temperature sensor n. 1 value, that is the reference for the alarms (not calibrated value).

The drawing sketch of the circuit realized for the alarm system is shown in Fig. 9. An interface is operative with the general security network inside the Gran Sasso underground laboratories. The alarm conditions, visual and acoustic in the installation, are therefore sent also to the general alarm system in order to allow a prompt intervening action. Seven alarms are connected: 1) lack of supply to the compressor unit; 2) failure of the compressor unit (internal sensors); 3) lack of insulation vacuum; 4) high pressure inside the Xenon vessel (P1 sensor); 5) high temperature of cooling water outgoing from the compressor unit (T1 sensor); 6) high temperature of the cryogenic set-up room or in the electronic set-up room (T2, T3 sensors); 7) failure of cooling water plant.

6 Conclusions

In this work we have described the main features of the low background DAMA pure liquid Xenon scintillator running deep underground in the Gran Sasso National Laboratory of I.N.F.N.

It has already achieved several physical results on the searches for various rare processes. Further data taking is in progress.

7 Acknowledgements

We thank the LNGS laboratory of the I.N.F.N. for support. We thank Mr. F. Bronzini, S. Parmeggiano and G. Ranelli for their qualified technical help, the INFN Sezione di Roma and INFN Sezione di Roma2 mechanical and electronical staffs for support and the ACF staff for hardware works and assistance.

We wish to thank Dr. M. Angelone, Dr. P. Batistoni and Dr. M. Pillon for their effective collaboration in the neutron measurements at ENEA-Frascati and Dr. C. Arpesella and Ing. M. Balata for their contribution to measurements on samples and gases. It is also a pleasure to thank Prof. E. Fiorini and the Mibeta group for making available to us the Xenon enriched in ^{136}Xe . Finally, we are indebt with Prof. S. d'Angelo for many stimulating discussions.

References

- [1] P. Belli et al., *Il Nuovo Cim.* 103A (1990) 767.
- [2] P. Belli et al., *Nucl. Instr. and Meth.* A316 (1992) 55; *Nucl. Instr. and Meth.* A336 (1993) 36; *Nucl. Phys.* B35(Proc. Sup.) (1993) 165; *Proc. The Dark side of the Universe*, World Sc. (1993) 257; *Proc. The Dark side of the Universe*, World Sc.(1995) 177; *Proc. ICRC95* vol.II (1995), 865.
- [3] R. Bernabei et al., *Phys. Lett. B* 436 (1998) 379.
- [4] P. Belli et al., *Il Nuovo Cim.* C19 (1996) 537.
- [5] R. Bernabei et al. *Phys. Lett.* B387 (1996) 222 and *Phys. Lett.* B389(1996) 783.
- [6] R. Bernabei et al., *New Journal of Phys.* 2 (2000) 15.1-15.7, (www.njp.org).
- [7] P. Belli et al., *Astroparticle Phys.* 5(1996) 217.
- [8] P. Belli et al., *Phys. Lett.* B465 (1999) 315.
- [9] P. Belli et al., *Phys. Rev.* D61 (2000) 117301.
- [10] R. Bernabei et al., *Phys. Lett.* B493 (2000) 12.
- [11] T. Doke, *Portugal Phys.* 12 (1980) 9.
- [12] A. Incicchitti et al., *Nucl. Instr. and Meth.* A289 (1990) 236.
- [13] J. Jortner et al., *J. Chem. Phys.* 42 (1965) 4250; N. Schwentner, E.E. Koch and J. Jortner, *Electronic Excitations in Condensed Rare Gases* (Springer, 1985).
- [14] B. Meyer, *Low Temperature Spectroscopy* (Elsevier, New York, 1971).

- [15] J.A. Northrop et al., IRE Trans. Nucl. Sci. NS-5 (1958) 81; J.A. Northrop and J.M. Grusky Nucl. Instr. and Meth. 3 (1958) 207.
- [16] S. Kubota et al. J. Phys., C11 (1978) 2645; Nucl Instr. & Meth. 196 (1982) 101; Nucl Instr. & Meth. A242 (1986) 291.
- [17] T.Doke et al., Nucl. Instr. and Meth. A291 (1990) 617.
- [18] S. Kubota et al., Phys. Rev. 17 (1978) 2762.
- [19] K. Masuda, talk given at the Conf. on Liquid Noble gas detectors and their applications, Stockolm, August 21-23, 1991.
- [20] M. Miyajima et al., Nucl. Instr. and Meth. B63 (1992) 297.
- [21] T. Doke and K. Masuda, *SPIE Proc.* vol. 305, (1994) 19.
- [22] G. J. Davies et al., Phys. Lett. B320 (1994) 395.
- [23] L. Lavoie, Medical Phys., 3 (1976) 283.
- [24] A. Braem et al. Nucl. Instr. and Meth. A320 (1992) 228.
- [25] E. Aprile et al. IEEE Trans. Nucl. Sci. NS-37(2) (1990) 553.
- [26] J. Seguinot et al., Nucl. Instr. and Meth. A323 (1992) 583.
- [27] "Argon, Helium and Rare Gases", G.A. Cook ed., Interscience Publishers/New York/London, 1961, vol. I.
- [28] P. Belli et al., Il Nuovo Cim. A101 (1989) 959.
- [29] SAES Getters, Milano, Italy.
- [30] ISOTECH co., specifications.
- [31] M. Balata, private communication.
- [32] E. Bellotti et al., Phys. Lett. B266 (1991) 193; Nucl. Instr. and Meth. B62 (1992) 529.
- [33] ISRIM analysis and M. Balata, private communication.
- [34] PALL Italia, Milano, Italy.
- [35] M. Wojcik, Nucl. Instr. and Meth. B61 (1991) 8.
- [36] J. Lindhard et al., Mat-Fys. Medd. **33** (1963) 10.
- [37] K. Fushimi et al., Phys. Rev. C47 (1993) R425.

- [38] R. Bernabei et al., Phys. Lett. B389 (1996) 757.
- [39] M. Martone et al., J. Nucl. Mat. 212-215 (1994) 1661; M. Pillon et al., Fus. Engin. and Design 28 (1995) 683; M. Angelone et al., Rev. Sci. Instr. 67 (1996) 2189.
- [40] F. Arneodo et al., Nucl. Instr. and Meth. A449 (2000) 147.
- [41] R. Luscher et al., IDM2000, York, Sept. 2000.
- [42] D.B. Cline, Nucl. Instr. and Meth. A327 (1993) 178 and ref. therein.